HHS Public Access

Author manuscript

Clin Imaging. Author manuscript; available in PMC 2017 May 01.

Published in final edited form as:

Clin Imaging. 2016 ; 40(3): 498–505. doi:10.1016/j.clinimag.2015.11.024.

Testing a dual-modality system that combines full-field digital mammography and automated breast ultrasound

Christopher L Vaughan[a,b,*], **Tania S Douglas**[a,b], **Qonita Said-Hartley**[c], **Roland V Baasch**[a], **James A Boonzaier**[a], **Brian C Goemans**[a], **John Harverson**[a], **Michael W Mingay**[a], **Shuaib Omar**[a], **Raphael V Smith**[a], **Nielen C Venter**[a], and **Heidi S Wilson**[a]

[a] CapeRay Medical (Pty) Ltd, Suite 2, 51 Bell Crescent, Westlake Business Park, Western Cape 7945, South Africa

[b] MRC/UCT Medical Imaging Research Unit, Faculty of Health Sciences, University of Cape Town, Observatory, Western Cape 7925, South Africa

[c]Department of Radiology, Groote Schuur Hospital, Observatory, Western Cape 7925, South Africa

Abstract

Purpose—The aim of this study was to test a novel dual-modality imaging system that combines full-field digital mammography (FFDM) and automated breast ultrasound (ABUS) in a single platform. Our Aceso system, named after the Greek goddess of healing, was specifically designed for the early detection of cancer in women with dense breast tissue.

Materials and Methods—Aceso was first tested using two industry standards: a CDMAM phantom as endorsed by EUREF was used to assess the FFDM images; and the CIRS 040GSE ultrasound phantom was imaged to evaluate the quality of the ABUS images. In addition, 58 women participated in a clinical trial: 51 were healthy volunteers aged between 40 and 65, while 7 were patients referred by the breast clinic, 6 of whom had biopsy-proven breast cancer.

Results—The CDMAM tests showed that the FFDM results were “acceptable” but fell short of “achievable” which was attributed to the low dose used. The ABUS images had good depth penetration (80 mm) and adequate axial resolution (0.5 mm) but the lateral resolution of 2 mm was judged to be too coarse. In a 42-year old volunteer with extremely dense breast tissue, the ABUS modality detected a lesion (a benign cyst) that was mammographically occult in the FFDM image. For a 73-year old patient with fatty breasts, a malignant lesion was successfully detected and co-registered in the FFDM and ABUS images. On average, each woman spent less than 11 minutes in the acquisition room.

[*]Corresponding Author, kit@caperay.com, web: http://www.caperay.com/, Tel: + 27 21 702 4299.

Conflicts of interest: CLV and TSD are board members and shareholders in CapeRay. QSH has no conflict of interest. RVB, JAB, JH, SO and HSW are employees and shareholders in CapeRay. BCG, MWM, RVS and NCV are engineering contractors to CapeRay.

Conclusions—While there is room for improvement in the quality of both the FFDM and ABUS images, Aceso has demonstrated its ability to acquire clinically meaningful images for a range of women with varying breast densities and therefore has potential as a screening device.

Keywords

ABUS; FFDM; Dual-modality imaging; Dense breasts; Breast cancer; Screening

1. Introduction

There is strong clinical evidence to support the screening of women for breast cancer [1] despite recent reports to the contrary [2, 3]. The traditional imaging modality for screening has been mammography although more recently other modalities, such as ultrasound and magnetic resonance imaging have been found to serve as useful adjuncts [4]. The sensitivity of full-field digital mammography (FFDM) for the detection of breast cancer varies from 75% to 90%, while the specificity varies from 90% to 95% [5]. One of the shortcomings of traditional X-ray mammography is that it performs poorly when the breasts are dense – often the case for younger women who are less than 50 years of age – and the sensitivity falls to less than 50% [6].

Although ultrasound does not have the spatial resolution of X-rays, it distinguishes tissues of different densities very well and has been used as an adjunct to X-ray mammography for more than fifty years [7]. In fact, diagnostic breast ultrasound now plays a vitally important role in the detection of cancer in both young and older women [8], while studies based on large cohorts have shown that hand-held ultrasound (done in addition to X-ray mammography) has resulted in a significant increase in the breast cancer detection rate [9 – 11]. Since hand-held ultrasound suffers from repeatability problems, automated breast ultrasound (ABUS) devices, where the patient lies on a bed in a supine position and her breasts are naturally compressed under the influence of gravity, have been developed [12] and tested [13]. With ABUS, the radiographer places the transducer assembly on the breast and a B-mode ultrasound probe scans across the breast in the frontal plane, producing 3D volumetric information.

The strongest evidence to date supporting the use of FFDM followed by ABUS as a screening tool has recently been published by Giuliano and Giuliano [14]. In a study of 3,418 women with mammographically dense breasts, the authors showed that the addition of ABUS resulted in the detection of 12.3 per 1,000 breasts cancers compared to 4.6 per 1,000 by mammography alone. Sensitivity increased from 76.0% to 97.7% while specificity increased from 98.2% to 99.7%. The potential for combining mammography and ultrasound was first hinted at thirty years ago during the analogue imaging era [15]. From a clinical point of view, a screening instrument that acquired both FFDM and ABUS images would make a significant contribution to the detection of breast cancer.

The ideal functional attributes of a dual-modality system should include: (1) breast to be in same orientation and degree of compression when X-ray and ultrasound images are obtained; (2) both sets of images to be acquired simultaneously so as to minimize the time the woman's breast is held stationary; (3) automated breast ultrasound that images the whole

breast in a single scan; (4) both modalities to acquire images in three dimensions (3D); and (5) radiation dose exposure to the woman is minimized. In reviewing the field of dual-modality imaging – combining X-rays and ultrasound – there are four basic design concepts that have been described in the literature.

In design one, X-ray images are captured by a flat panel digital detector located beneath the breast and an ultrasound probe located above the breast [16 – 18]. This probe, which is moved under automated control on top of the compressor, is positioned between the X-ray tube and the breast. Because flat-panel detectors suffer from scatter problems [19], the radiation exposure to the patient is higher than optimal. In design two, researchers from the University of Michigan and GE Healthcare have essentially adapted design one and added digital breast tomosynthesis (DBT), a technology that enables 3D images of the breast to be reconstructed [20 – 24]. In a study of 51 patients with biopsy-proven masses, Padilla *et al.* [25] found no significant difference in receiver operating characteristic (ROC) performance when ABUS was added to DBT.

Design three is based on an FFDM system that uses a slot-scanning approach to acquire a planar X-ray image [26]. Since the X-ray detector moves beneath the breast platform, it is possible to locate the ultrasound probe parallel to the X-ray detector [27 – 28]. Because the detector and the probe are both beneath the breast platform it is possible to acquire the two images simultaneously, while the slot-scanning geometry reduces scatter and therefore minimizes radiation exposure to the patient [29]. The researchers were unable to solve the problem of acoustically coupling the probe to the breast but they were able to co-register the FFDM and ABUS images [30]. Design four requires the patient to lie on her stomach in a prone position with her breast protruding through an opening in the horizontal support [31]. Both the X-ray and ultrasound acquisition systems are located beneath the support and rotate around the breast, enabling the capture of 3D images in both modalities. Although the method of acquiring 3D X-ray images could expose the patient to an unnecessarily high radiation dose [32], Koning recently received FDA approval for their breast CT system based on a clinical trial [33].

2. Materials and Methods

2.1 System overview

Our dual-modality Aceso system, named after the Greek goddess of healing, is based on design concept three, where FFDM is implemented using a slot-scanning approach [34], and ABUS is accomplished by locating the ultrasound transducer parallel to the X-ray detector [35]. Our slot-scanning geometry differs from the Fischer system [26 – 28] in that the X-ray tube is stationary and a moving collimator sweeps the fan beam across the field of view [35]. As seen in Figure 1, Aceso consists of: an acquisition workstation that includes an X-ray generator, an iPad as the user interface, and a lead-shielded glass screen; a pair of wireless foot pedals; a gantry that includes an ultrasound beam former and a Mac Mini system computer; and a C-arm that houses an X-ray tube, a display screen, an instrumented compression paddle, and a hermetically-sealed breast platform (HSBP). Photographs of the Aceso system, as used in the clinical trial, are seen in Figure 2.

The HSBP accommodates both the digital X-ray camera and the ultrasound transducer that are able to move independently on two separate rail carriages. Both the camera and the transducer, together with two motors controlling their movement, are immersed in mineral oil in the HSBP [36]. This fluid, together with the upper surface of the HSBP that is made from 6 mm thick TPX [23], is designed to enhance the acoustic coupling between the ultrasound transducer and the breast. The size of the TPX plate is 230 mm in the anterior direction (i.e. away from the patient's chest wall) by 285 mm in the medio-lateral (i.e. scanning) direction. The custom-designed camera, which is hermetically sealed, utilizes a CCD sensor (8,160 × 256 pixels, with a pixel size of 27 μm) and operates in time-delayed integration (TDI) mode [26]. The ultrasound transducer is 128 mm in length, has an element pitch of 1 mm (i.e. there are 128 elements) and a centre frequency of 3.5 MHz. The centre lines of the X-ray camera and the ultrasound transducer are offset by 20 mm.

A right-handed coordinate system is used: the x-axis is in the anterior direction, the y-axis is from right to left, while the z-axis is upward and orthogonal to the breast platform. The origin of the system is located at the first pixel of the X-ray camera when the camera is in its home position (see Figure 3). When dual-modality mode is implemented, the ultrasound transducer begins to move first at a constant speed of 10 mm/s, acquiring B-mode images of the breast in the sagittal (x-z) plane at intervals of 1 mm. As the ultrasound transducer reaches approximately three-quarters of the way along its track (at 150 mm, reached after 15 s), the X-ray camera begins to move at a constant speed of 40.5 mm/s, acquiring its image of the breast in the horizontal (x-y) plane. Thus, for the final 6 to 8 seconds of image acquisition, the two modalities are operating simultaneously, meaning that the total acquisition time is limited to 25 seconds. There are 230 ABUS images gathered in a single scan (field of view 128 mm x 89 mm, recorded as an 8-bit gray scale image of 810 × 562 pixels), and a single FFDM image (field of view 224.1 mm × 220.3 mm, recorded as a 16-bit gray scale image of 4150 × 4080 pixels). All images are saved in standard DICOM format with header information that enables the ABUS and FFDM images to be co-registered using the coordinate system defined in Figure 3.

2.2 Phantom Testing

Two phantoms were used for evaluating the dual-modality Aceso system prior to clinical testing: the CDMAM test object for assessing digital mammography systems that is manufactured by Artinis Medical Systems (Einsteinweg 17, Elst, The Netherlands); and the Model 040GSE multi-tissue ultrasound phantom manufactured by CIRS (2428 Almeda Avenue, Norfolk VA, USA). The CDMAM phantom is part of the European guidelines for image quality control in mammography [37] and involves the determination of threshold contrast visibility using gold disks of different thicknesses (between 2.0 and 0.03 μm) and a range of diameters (between 2.0 and 0.06 mm). Software to process the CDMAM images is freely available from the EUREF website (www.euref.org). The CIRS Model 040GSE phantom is constructed from Zerdine, which simulates the acoustic properties of soft human tissue, and consists of: a series of wire targets that are made from nylon of diameter 0.1 to 0.08 mm and appear as bright dots; gray scale disks to assess contrast sensitivity at two depths; elasticity targets with a range of stiffnesses from 10 to 60 kPa; and anechoic stepped cylinders to mimic small cysts.

2.3 Subjects

Fifty-one healthy volunteer subjects were recruited through the human resources department of the University of Cape Town (UCT). A further seven patients, six with biopsy-confirmed breast cancer, were recruited through the breast clinic at Groote Schuur Hospital. The study was approved by the Human Research Ethics Committee of UCT's Faculty of Health Sciences and written, informed consent was obtained from all subjects prior to participation in the study. The volunteers were aged between 40 and 65 and had no prior history of breast disease. Each subject had four sets of dual-modality images acquired: cranio-caudal (CC) and medio-lateral oblique (MLO) views for the left and right breasts.

For each of the 58 subjects, the radiologist (QSH) compared the Aceso FFDM images with a predicate device used in her own practice at Groote Schuur Hospital (GE system with Agfa CR detector). Note that she did not have images of the same patient for a side-by-side comparison. There were 12 parameters (Table 1), based on the FDA guidelines that were compared: breast positioning (cranio-caudal and medio-lateral oblique); exposure (adipose, fibroglandular and pectoralis); breast compression; image contrast; sharpness; tissue visibility; noise; artifacts; and image quality (www.fda.gov/RegulatoryInformation/Guidances/ucm107552.htm). Each parameter, for each subject, was given one of three scores: −1 was recorded if Aceso was worse than the predicate system; 0 if the two systems were equivalent; and +1 if Aceso was judged to be better than the predicate. In addition, each subject's breast density was scored according to the Breast Imaging – Reporting and Data System (BI-RADS): 1 = almost entirely fatty; 2 = scattered fibroglandular densities; 3 = heterogeneously dense; and 4 = extremely dense. Finally, the total time that each subject was in the room for image acquisition was recorded.

3. Results

3.1 Phantom testing

The CDMAM phantom (serial number 1809, version 3.4) was positioned on the breast platform with a 20 mm thickness of polymethylmethacrylate (PMMA) above and below, thus providing a total attenuation equivalent to 50 mm of PMMA or approximately 60 mm of breast tissue. With a W/Al target/filter combination, X-ray tube values of 33 kV and 31 mAs were chosen, based on automatic exposure control (AEC) values for 50 mm thickness of PMMA, while a mean glandular dose (MGD) of 2.1 mGy was estimated using the method of Dance *et al.* [38]. Eight consecutive images of CDMAM were acquired and the resulting DICOM files were fed into the EUREF software package. Figure 4 illustrates the system performance where, in logarithmic scale, the threshold gold thickness (in μm) is plotted as a function of detail diameter (in mm). The average curve for Aceso may be compared to the EUREF standards of “acceptable” and “achievable” [37].

The CIRS 040GSE ultrasound phantom was located on the breast platform on top of a 2 mm Zerdine sheet and the ultrasound probe was scanned in the +y direction (see Figure 3). The template for the targets is shown in Figure 5(a), while a single slice in the sagittal (x-z) plane of the phantom structures may be seen in Figure 5(b). Based on the two images in Figure 5, the resolution in the lateral (x) direction was approximately 2 mm, while the axial (z-axis)

resolution was 0.5 mm. The acquisition spacing in the scanning (y) direction was 1 mm. The depth penetration in the axial (z) direction was 80 mm, while the full range of the gray scale (from −9 to +6 dB) could be discerned, as could the hyperechoic mass. The elasticity targets were poorly imaged while those in the far field produced significant artifacts for the 10 kPa elasticity.

3.2 All subjects

The average age for our subjects was 50.4 years (Table 2), with a range of 36 to 73 where the two outliers were patients (all volunteers were aged between 40 and 65). The breast density data for the 58 subjects are illustrated in Figure 6, where 19 women (33%) were judged to have heterogeneously or extremely dense breasts (BI-RADS 3 and 4). The largest group of 35 women had scattered fibroglandular densities (BI-RADS 2). For all 12 of the FFDM parameters defined in Table 1, Aceso's performance was judged to be inferior to the predicate system (Table 2). For some of the parameters (*e.g.* breast positioning for the CC view and noise) the differences were negligible, but for others (*e.g.* sharpness and tissue visibility) the differences were marked.

The average time spent by the 58 women in the imaging room was 10 minutes and 57 seconds (Table 2). The range was 8:50 to 14:55 although there was clearly a training effect for the radiographer, because in the latter part of the trial most women spent less than 10 minutes in the imaging room.

For the seven patients, the radiologist (QSH) recorded her findings for the FFDM and ABUS images generated by Aceso. In addition, the breast density (BI-RADS 1 to 4) was also recorded for each patient (see Table 3). One of the patients (number 3, who had extremely dense tissue) was deemed to have no breast pathology. The radiologist was aware that the other six patients had biopsy-proven cancer but she did not have access to any prior images.

3.3 Volunteer with dense breast tissue

Three of our subjects had extremely dense breast tissue (Figure 6) and we feature here a 42-year old healthy volunteer with BI-RADS 4 and no prior history of breast pathology. Figure 7 shows an FFDM image for the left medio-lateral oblique (LMLO) view where the radiologist (QSH) confirmed there was no evidence of breast pathology. The 230 ABUS images were acquired simultaneously to the FFDM image in the sagittal (x-z) plane and may be viewed as a video clip. This animation revealed the brief appearance of a dark well-defined lesion close to the breast platform about half way through the video.

Because the location of the probe in the +y direction is known, a 3D reconstruction of the ABUS data was performed. As seen in Figure 8, the four views illustrate the co-registration of the FFDM and ABUS images generated by Aceso. This figure was created using the open source 3D Slicer software package (www.slicer.org). Note that the 3D location of the lesion is clearly identified by the crosshairs in the three orthogonal planes of the ABUS image: sagittal, coronal and horizontal. However, in the FFDM image (bottom right), the lesion is occult, even to the experienced radiologist. Fortunately for this volunteer, who was referred for follow-up evaluation, the lesion was identified as a benign cyst.

3.4 Patient with malignant lesion

Figure 9 shows an FFDM image of the right medio-lateral oblique (RMLO) view for a 73-year old patient with a prior history of cancer in the left breast that was treated by lumpectomy (patient number 1 in Table 3). An irregular-shaped mass is clearly visible in the right lower quadrant that was confirmed as malignant on biopsy. The video clip of the ABUS images, acquired at the same time as the FFDM image, illustrated the brief appearance of a large irregularly shaped lesion located midway between the breast platform and the upper surface of the breast.

As seen in Figure 10, the four views illustrate the co-registration of the FFDM and ABUS images generated by Aceso. Note that the 3D location of the lesion is clearly identified by the crosshairs in the three orthogonal planes of the ABUS image. This large irregular-shaped malignant lesion is co-registered in the horizontal plane of the FFDM image (bottom right).

4. Discussion

The purpose of this study was to test our dual-modality Aceso system that combines full-field digital mammography (FFDM) and automated breast ultrasound (ABUS) in a single platform, and in particular to evaluate how it performed in a clinical setting. All testing was conducted at the University of Cape Town's Lung Institute, and took place over a period of four weeks, with a maximum of six women seen on a single day. On average, image acquisition took less than 11 minutes per subject (Table 2), with this time being less than 10 minutes in the second half of the study. Aceso used breast compressions up to a maximum of 50 Newton for the combined FFDM and ABUS images, which is considerably lower than the 100 to 150 Newton used in most FFDM systems. For those subjects who had previously had a mammogram, the majority provided positive subjective feedback, while among the negative comments mentioned was that the ultrasound gel used to acoustically couple the breasts to the TPX platform had to be wiped clean after the study.

The quality of the FFDM images may be gauged from Figure 4, Table 2, and Figures 7 and 9. As seen in Figure 4, the curve for Aceso falls almost exactly on the “acceptable” curve published by EUREF [37]. However, as highlighted in Table 2, Aceso's performance was judged to be inferior to the predicate device for all 12 of the FDA parameters based on the clinical images. We believe there are two primary reasons for this poor performance. First, in an effort to keep the radiation exposure to the subjects as low as possible, we used a relatively low mean glandular dose. By using a higher but clinically acceptable dose in the region of 3.0 mGy, there would have been better exposure, thus leading to improved visualization of the adipose and fibroglandular tissues and the pectoral muscles, as well as better image contrast (cf. Table 2). Second, we had not optimized the post-processing algorithm for the captured images at the time they were read by the radiologist (QSH) and this led to poor scores for the sharpness and tissue visibility comparisons (Table 2). It should be noted that Figures 7(a) and 9(a) illustrate the images that were read by the radiologist (QSH), whereas Figures 7(b) and 9(b) are images to which the optimized post-processing algorithm has been applied. The improvement in the quality of the images is clearly visible.

The quality of the ABUS images may be gauged from Figures 5, 8 and 10. When the phantom data of Figure 5(b) are compared with the template in Figure 5(a), Aceso is able to image most, but not all of the targets. While the depth penetration of 80 mm is sufficient for imaging all breast sizes, and the axial (z-axis) resolution of 0.5 mm is acceptable, the lateral (x-axis) resolution of 2 mm is too coarse to detect small lesions. The “spreading” of the signal in the lateral direction is a function of the ultrasound transducer element pitch (1 mm), the centre frequency (3.5 MHz), and the refraction caused by the 6 mm thick TPX platform resulting from a mismatch in the speed of sound [39].

The lateral spreading of the ultrasound signals is also evident in the sagittal plane views of the healthy volunteer with dense breast tissue (Figure 8) and the patient with a malignant lesion (Figure 10). Aside from the lateral resolution, there are two other shortcomings with the ABUS images: first, since the ultrasound transducer was only 128 mm in length, it was not long enough to image large breasts with a single scan; and second, there is a “peripheral volume” problem, where the tissue on the periphery of the breast (laterally, medially and anteriorly under the nipple) is not in contact with the TPX platform. This latter problem is particularly evident in the lower two images of Figure 10, where the ABUS image in the horizontal plane has a significantly smaller footprint than the FFDM image in the same plane, where both images are reproduced to the same scale.

As seen in Table 3, Aceso's FFDM modality was used by the radiologist (QSH) to successfully identify the cancers in all 6 women with biopsy-proven malignancies. In 4 of these 6 patients, Aceso's ABUS images provided complimentary information, confirming the diagnosis and helping to characterize the lesion. For the one referred patient who had no pathology but very dense breasts (patient number 3), the FFDM images revealed no discrete spiculations or architectural distortions and no malignant micro-calcifications, while the ABUS images showed normal tissue with no visible solid or cystic masses. These findings suggest that Aceso has potential to be used in a screening environment although the image quality issues do still need to be addressed.

In order to improve the quality of the ABUS images, it will be necessary to implement three strategies: (1) increase the lateral resolution by building a transducer with a smaller pitch (0.2 to 0.5 mm) and a higher centre frequency (at least 6.5 MHz); (2) increase the length of the transducer so that it is closer in length to the X-ray transducer (approaching 200 mm); and (3) solve the peripheral volume problem by introducing a new system to acoustically couple more of the breast to the TPX platform. We are at present addressing each of these design challenges and will be testing a new version of Aceso in a clinical trial in the near future.

Although digital mammography is still recognized as the gold standard when screening for breast cancer, it is also acknowledged that when a woman has dense breast tissue, lesions may be mammographically occult. These false negative findings can have devastating consequences for the women concerned because a later diagnosis will often lead to more expensive treatment options and a poor prognosis. As seen in Figures 7 and 8, the Aceso system, which needs just ten minutes to acquire a full set of FFDM and ABUS images, was able to successfully detect and locate a mammographically occult lesion in a woman with

dense breast tissue. We believe that Aceso and its dual-modality technology have shown promise as a potential screening device.

Acknowledgments

We acknowledge the grant funding from the National Institutes of Health (R21 CA101705) for the early development of Aceso and the Cancer Association of South Africa (CANSA) that supported the clinical trial. We are also grateful to Natasha Steele for recruitment of the volunteers, Nafeesah Kariem who served as the clinical radiographer, Chipo Chimhundu who assisted with gathering informed consent, radiologist Dr Andrew du Toit and obstetrician Dr Helmut Schillinger who both provided feedback on the clinical images.

References

1. Weedon-Fekjær H, Romundstad PR, Vatten LJ. Modern mammography screening and breast cancer mortality: population study. British Medical Journal. 2014; 348:g3701. [PubMed: 24951459]
2. Bleyer A, Welch HG. Effect of three decades of screening mammography on breast-cancer incidence. New England Journal of Medicine. 2012; 367:1998–2005. [PubMed: 23171096]
3. Miller AB, Wall C, Baines CJ, Sun P, To T, Narod SA. Twenty five year follow-up for breast cancer incidence and mortality of the Canadian National Breast Screening Study: randomised screening trial. British Medical Journal. 2014; 348:g366. 2014. [PubMed: 24519768]
4. Kuhl CK, Schrading S, Strobel K, Schild HH, Hilgers R-D, Bieling HB. Abbreviated breast magnetic resonance imaging (MRI): first post-contrast subtracted images and maximum-intensity projection: a novel approach to breast cancer screening with MRI. Journal of Clinical Oncology. 2014; 32(22):2304–2310. [PubMed: 24958821]
5. Vaughan CL. New developments in medical imaging to detect breast cancer. Continuing Medical Education. 2011; 29(3):122–125.
6. Kelly KM, Dean J, Comulada WS, Lee S-J. Breast cancer detection using automated whole breast ultrasound and mammography in radiographically dense breasts. European Radiology. 2010; 20(3): 734–742. [PubMed: 19727744]
7. Dempsey PJ. The history of breast ultrasound. Journal of Ultrasound in Medicine. 2004; 23:887–894. [PubMed: 15292555]
8. Yang W, Dempsey PJ. Diagnostic breast ultrasound: current status and future directions. Ultrasound Clinics. 2009; 4:117–133.
9. Berg WA, Blume JD, Cormack JB, Mendelson EB, Lehrer D, Böhm-Vélez M, Pisana ED, Jong RA, Evans WP, Morton MJ, Mahoney MC, Larsen LH, Barr RG, Farria DM, Marques HS, Boparai K, for the ACRIN6666 Investigators. Combined screening with ultrasound and mammography vs mammography alone in women at elevated risk of breast cancer. Journal of the American Medical Association. 2008; 299(18):2151–2163. [PubMed: 18477782]
10. Nothacker M, Duda V, Hahn M, Warm M, Degenhardt F, Madjar H, Weinbrenner S, Albert US. Early detection of breast cancer: benefits and risks of supplemental breast ultrasound in asymptomatic women with mammographically dense breast tissue. A systematic review. BMC Cancer. 2009; 9:335. doi: 10.1186/1471-2407-9-335. [PubMed: 19765317]
11. Schaefer FKW, Waldmann A, Katalinic A, Wefelnberg C, Heller M, Jonat W, Schreer I. Influence of additional breast ultrasound on cancer detection in a cohort study for quality assurance in breast diagnosis – analysis of 102,577 diagnostic procedures. European Radiology. 2010; 20(5):1085–1092. [PubMed: 19890643]
12. Chou YH, Tiu CM, Chen J, Chang RF. Automated full-field breast ultrasonography: the past and the present. Journal of Medical Ultrasound. 2007; 15(1):31–44.
13. Arleo EK, Saleh M, Ionescu D, Drotman M, Min RJ, Hentel K. Recall rate of screening ultrasound with automated breast volumetric scanning (ABVS) in women with dense breasts: a first quarter experience. Clinical Imaging. 2014; 38:439–444. [PubMed: 24768327]
14. Giuliano V, Giuliano C. Improved breast cancer detection in asymptomatic women using 3D-automated breast ultrasound in mammographically dense breasts. Clinical Imaging. 2013; 37(3): 480–486. [PubMed: 23116728]

15. Novak D. Indications for and comparative diagnostic value of combined ultrasound and X-ray mammography. European Journal of Radiology. 1983; 3(Supplement 1):299–302. [PubMed: 6628417]

16. Shmulewitz A. Methods and apparatus for performing sonomammography. Dec.1995 (12) United States Patent and Trademark Office, Patent Number 5,474,072

17. Dines KA, Kelly-Fry E, Romilly AP. Mammography method and apparatus. Jun.2003 (3) United States Patent and Trademark Office, Patent Number 6,574,499

18. Entrekin RR, Change ND. Compression plate for diagnostic breast imaging. Jan.2004 (27) United States Patent and Trademark Office, Patent Number 6,682,484

19. Irving BJ, Maree GJ, Hering ER, Douglas TS. Radiation dose from a linear slit scanning xray machine with full-body imaging capabilities. Radiation Protection Dosimetry. 2008; 130(4):482–489. [PubMed: 18420566]

20. Kapur, A.; Krucker, J.; Astley, O.; Buckley, D.; Eberhard, JW.; Alyassin, AM.; Claus, BEH.; Thomenius, KE.; Myers, H.; Rumsey, M.; Johnson, RN.; Karr, S. Fusion of digital mammography with breast ultrasound: a phantom study. In: Antonuk, LE.; Yaffe, MJ., editors. Medical Imaging: Physics of Medical Imaging; Proceedings SPIE; 2002; p. 526-537.

21. Kapur A, Carson PL, Eberhard J, Goodsitt MM, Thomenius K, Lokhandwalla M, Buckley D, Roubidoux MA, Helvie MA, Booi RC, LeCarpentier GL, Erkamp RQ, Chan HP, Fowlkes JB, Thomas JA, Landberg CA. Combination of digital mammography with semiautomated 3D breast ultrasound. Technology in Cancer Research Treatment. 2004; 3(4):325–334. [PubMed: 15270583]

22. Booi RC, Krücker JF, Goodsitt MM, O'Donnell M, Kapur A, LeCarpentier GL, Roubidoux MA, Fowlkes JB, Carson PL. Evaluating thin compression paddles for mammographically compatible ultrasound. Ultrasound in Medicine and Biology. 2007; 33(3):462–482.

23. Sinha, SP.; Roubidoux, MA.; Helvie, MA.; Nees, AV.; Goodsitt, MM.; LeCarpentier, GL.; Fowlkes, JB.; Chalek, CL.; Carson, PL. Multi-modality 3D breast imaging with X-ray tomosynthesis and automated ultrasound. Proceedings of the 29th International Conference of the IEEE EMBS; Lyon, France. 23-26 August 2007; p. 1335-1338.

24. Goodsitt, MM.; Chan, HP.; Hadjiiski, L.; LeCarpentier, GL.; Carson, PL. Automated registration of volumes of interest for a combined x-ray tomosynthesis and ultrasound breast imaging system. In: Krupinski, EA., editor. Digital Mammography. Springer-Verlag; Berlin: p. 463-468, 2008.Lecture Notes in Computer Science 5116

25. Padilla F, Roubidoux MA, Paramagul C, Sinha SP, Goodsitt MM, Le Carpentier GL, Chan HP, Hadjiiski LM, Fowlkes JB, Joe AD, Klein KA, Nees AV, Noroozian M, Patterson SK, Pinsky RW, Hooi FM, Carson PL. Breast mass characterization using 3-dimensional automated ultrasound as an adjunct to digital breast tomosynthesis: a pilot study. Journal of Ultrasound in Medicine. 2013; 32(1):93–104. [PubMed: 23269714]

26. Tesic MM, Piccaro MF, Munier B. Full field digital mammography scanner. European Journal of Radiology. 1999; 31:2–17. [PubMed: 10477093]

27. Besson GM, Nields MW. Integrated X-ray and ultrasound medical imaging system. Jan.2005 (25) United States Patent and Trademark Office, Patent Number 6,846,289

28. Suri J, Janer R, Guo Y Elbakri I. Diagnostic system for multimodality mammography. Mar.2011 (29) United States Patent and Trademark Office, Patent Number 7,916,918

29. Lease, A.; Vaughan, CL.; Beningfield, SJ.; Potgieter, JH.; Booysen, A. Feasibility of using Lodox technology for mammography. In: Antonuk, LE.; Yaffe, MJ., editors. Medical Imaging: Physics of Medical Imaging; Proceedings SPIE; 2002; p. 656-664.

30. Suri, JS.; Danielson, T.; Guo, Y.; Janer, R. Fischer's fused full field digital mammography and ultrasound system (FFDMUS). In: Bos, L., editor. Medical and Care Compunetics 2. IOS Press; p. 177-200, 2005.

31. Li B, Thibault JB, Hall AL. Combining X-ray and ultrasound imaging for enhanced mammography. Nov.2010 (9) United States Patent and Trademark Office, Patent Number 7,831,015

32. Boone JM, Nelson TR, Lindfors KK, Seibert JA. Dedicated breast CT: radiation dose and image quality evaluation. Radiology. 2001; 221(3):657–667. [PubMed: 11719660]

33. O'Connell A, Conover DL, Zhang Y, Seifert P, Logan-Young Y, Lin C-FL, Sahler L, Ning R. Cone-beam CT for breast imaging: radiation dose, breast coverage, and image quality. American Journal of Roentgenology. 2010; 195:496–509. [PubMed: 20651210]

34. Hussein K, Vaughan CL, Douglas TS. Modeling, validation and application of a mathematical tissue-equivalent breast phantom for linear slot-scanning digital mammography. Physics in Medicine and Biology. 2009; 54(6):1533–1553. [PubMed: 19229099]

35. Vaughan CL, Evans MD. Diagnosing breast cancer: an opportunity for innovative engineering. South African Medical Journal. 2012; 102(6):562–564. [PubMed: 22668964]

36. Evans, MD.; Smith, RV.; Vaughan, CL. Dual-modality mammography. United Kingdom Patent Office, Patent Number 2509193. Jul. 2015

37. Young, KC.; Abdulaaziz, A.; Oduko, JM.; Bosmans, H.; Verbrugge, B.; Geertse, T.; van Engen, R. Evaluation of software for reading images of the CDMAM test object to assess digital mammography systems. Medical Imaging 2008: Physics of Medical Imaging; Proceedings of SPIE; doi: 10.1117/12.770571, 2008

38. Dance DR, Young KC, van Engen RE. Further factors for the estimation of mean glandular dose using the United Kingdom, European and IAEA breast dosimetry protocols. Physics in Medicine and Biology. 2009; 54(14):4361–4372. [PubMed: 19550001]

39. Chen Q, Zagzebski JA. Simulation study of effects of speed of sound and attenuation on ultrasound lateral resolution. Ultrasound in Medicine and Biology. 2004; 30(10):1297–1306. [PubMed: 15582229]

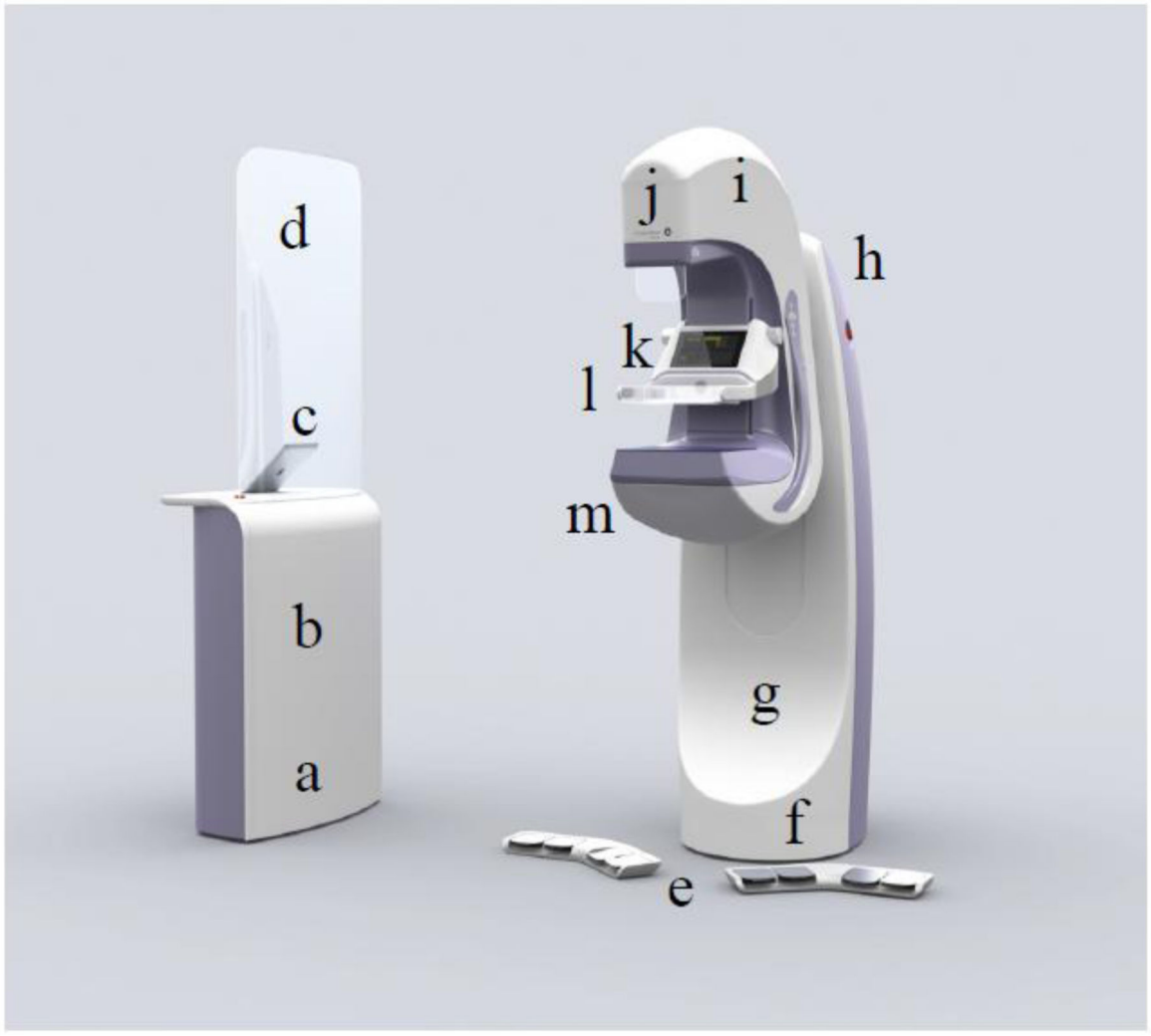

Figure 1.

The Aceso dual-modality imaging system consists of: (a) an acquisition workstation that includes (b) an X-ray generator, (c) an iPad as the user interface, and (d) a lead-shielded glass screen; (e) a pair of wireless foot pedals; (f) a gantry that includes (g) an ultrasound beam former and (h) a Mac Mini system computer; and (i) a C-arm that houses (j) an X-ray tube, (k) a display screen, (l) an instrumented compression paddle, and (m) a hermetically-sealed breast platform (HSBP). The HSBP incorporates both the digital X-ray camera and the linear ultrasound transducer submerged in mineral oil.

Figure 2.
The Aceso dual-modality system as installed at the University of Cape Town for the clinical trial: (a) complete system; and (b) view as seen by the patient, showing the digital X-ray camera and the ultrasound transducer in the home position.

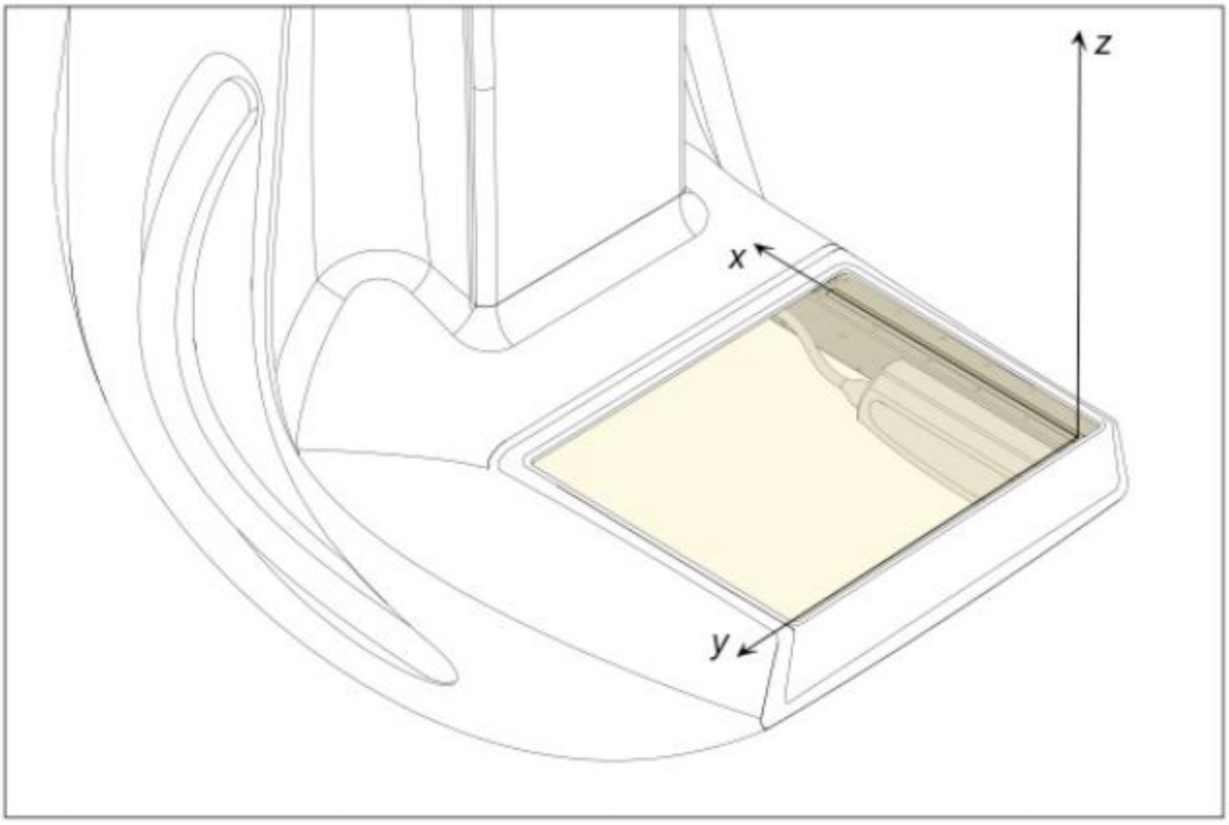

Figure 3.
Definition of the Aceso's three-dimensional coordinate system, showing the origin embedded at pixel 1 of the digital X-ray camera. Note that the camera and ultrasound transducer are parallel to one another, with the transducer offset by 22 mm in the y direction.

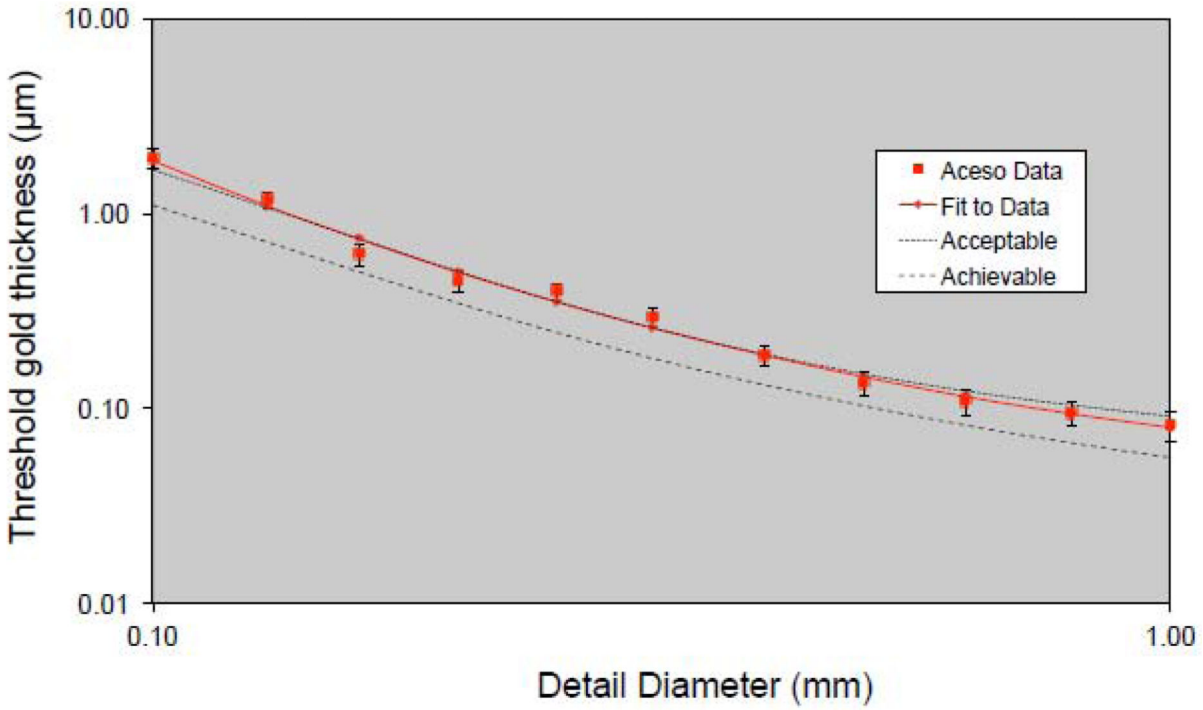

Figure 4.

Data for the CDMAM phantom generated by the EUREF software package (www.euref.org). The threshold gold thickness has been plotted as a function of detail diameter, with both axes using a logarithmic scale. The Aceso data are based on eight sequential X-ray images (at 31 kV, 27 mAs, 2.1 mGy) and may be compared with the EUREF standards of “acceptable” and “achievable” [37].

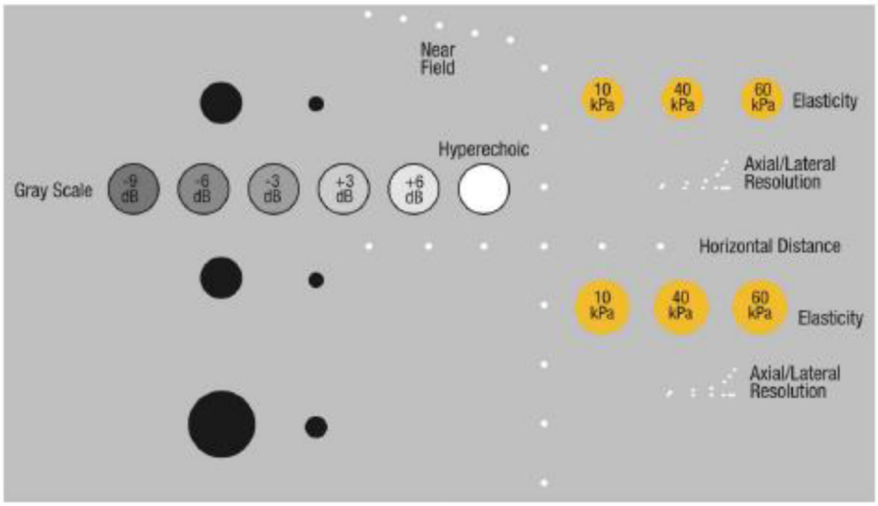

(a)

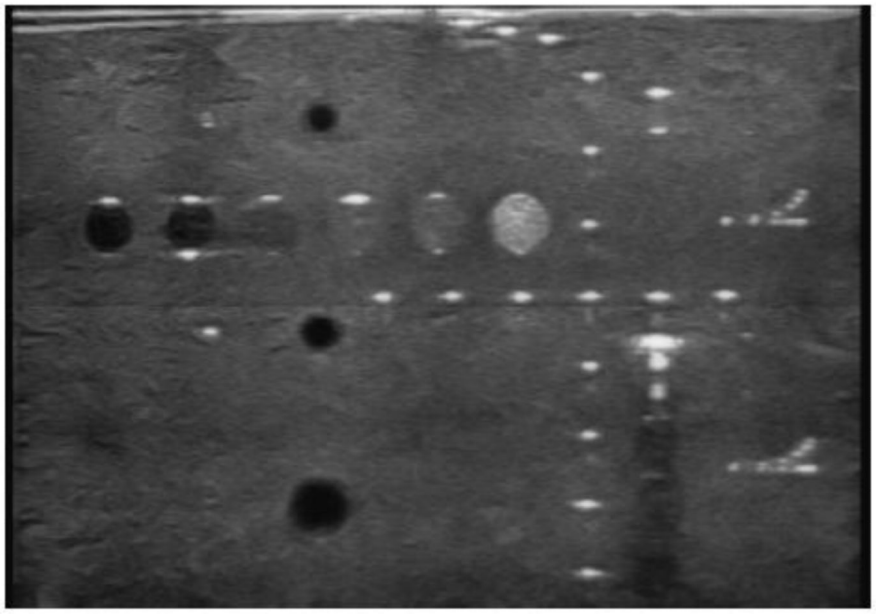

(b)

Figure 5.
The CIRS 040GSE ultrasound phantom: (a) template showing the various targets; and (b) data captured by the ultrasound transducer during the clinical trial.

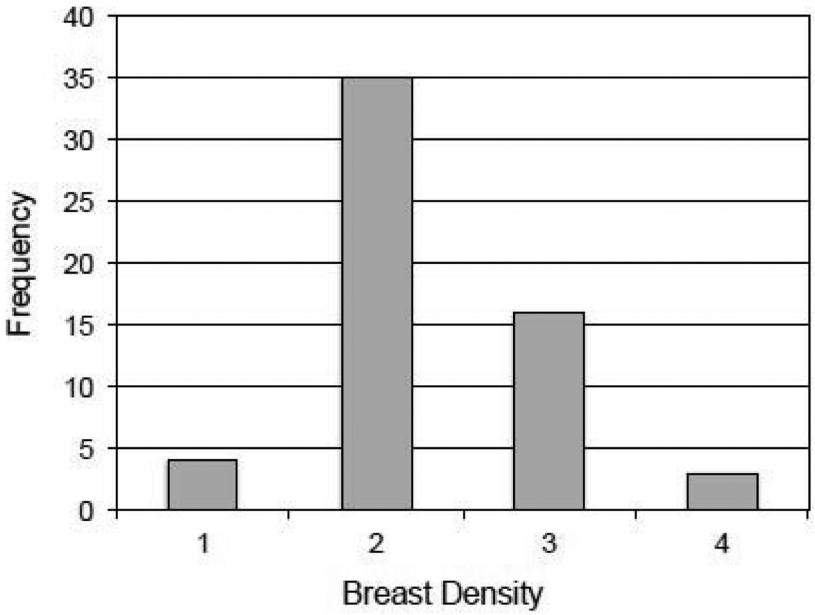

Figure 6.
The distribution (i.e. frequency) of the 58 subjects by breast density using the BI-RADS scale that ranges from 1 to 4.

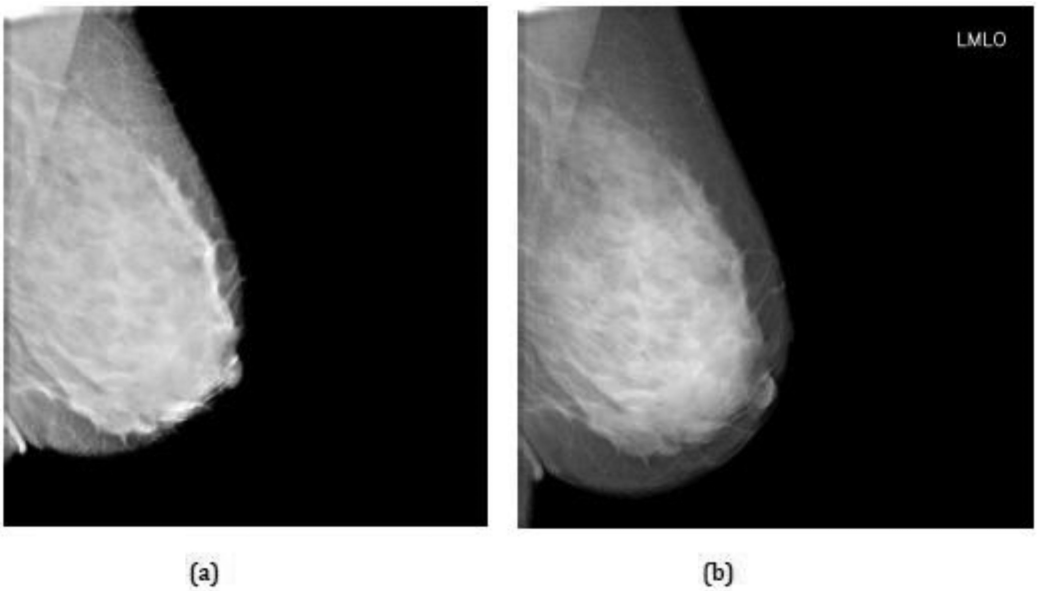

Figure 7.
Full-field digital mammogram (FFDM) of the left medio-lateral oblique (LMLO) view for a 42-year old healthy volunteer with BI-RADS 4 breast density: (a) before; and (b) after implementation of an optimized post-processing algorithm. Note that there is no evidence of a lesion.

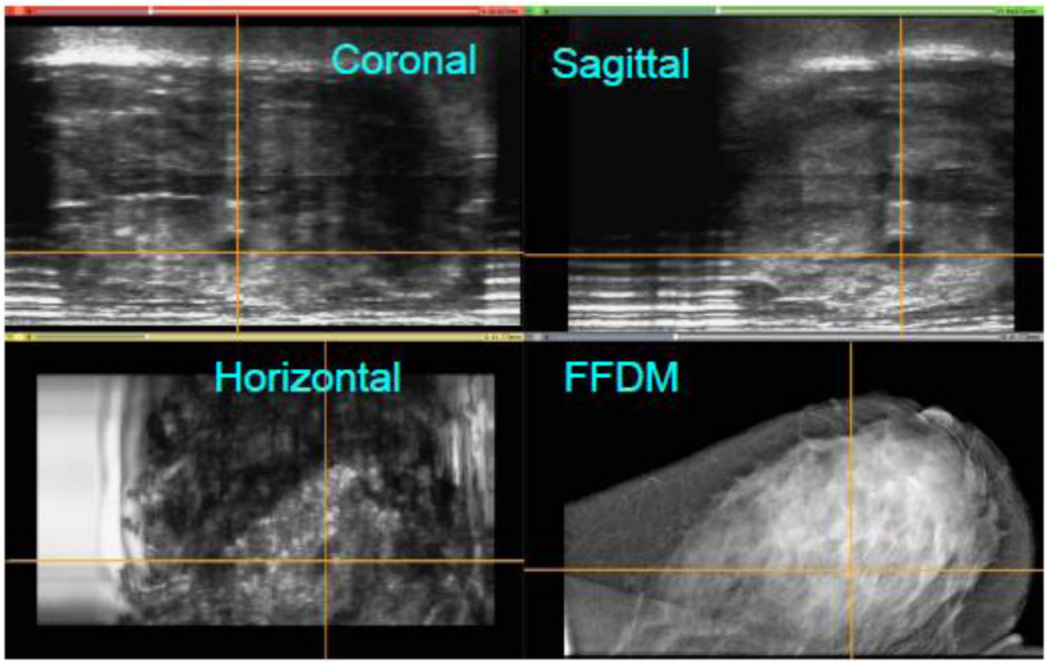

Figure 8.

Co-registration of the full-field digital mammogram (FFDM) in the horizontal plane and the automated breast ultrasound (ABUS) images in the horizontal, coronal and sagittal planes. A lesion (benign cyst) has been highlighted by cross hairs in the ABUS views. The lesion is occult in the FFDM image. Note that for the ABUS images, the sagittal plane view is the acquired image, whereas the coronal and horizontal plane views have been reconstructed.

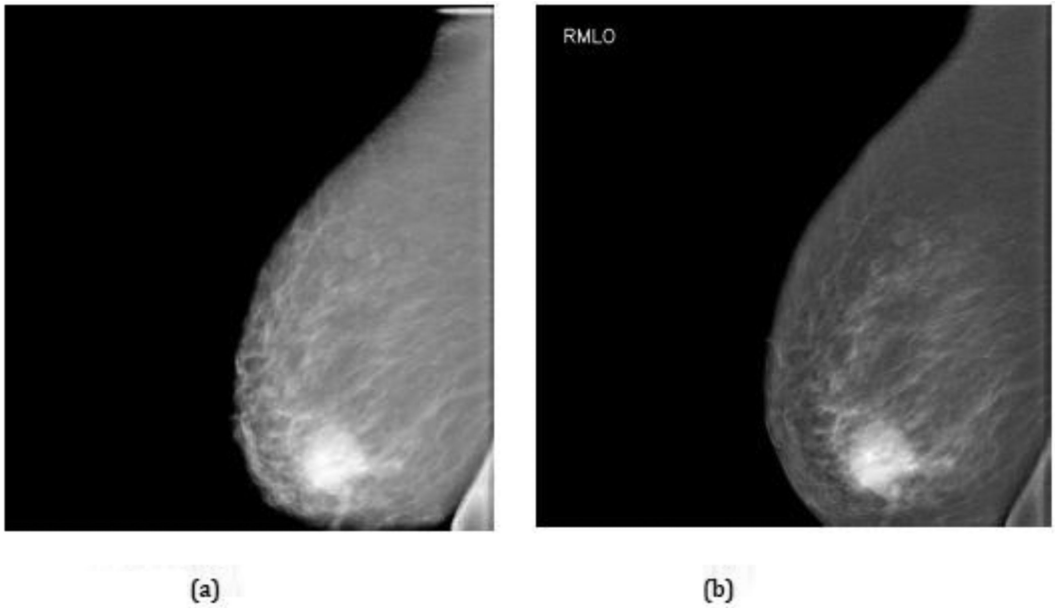

Figure 9.

Full-field digital mammogram (FFDM) of the right medio-lateral oblique (RMLO) view for a 73-year old patient with a prior history of cancer in the left breast: (a) before; and (b) after implementation of an optimized post-processing algorithm. Note the irregularly shaped mass in the right lower quadrant that was confirmed as malignant at biopsy.

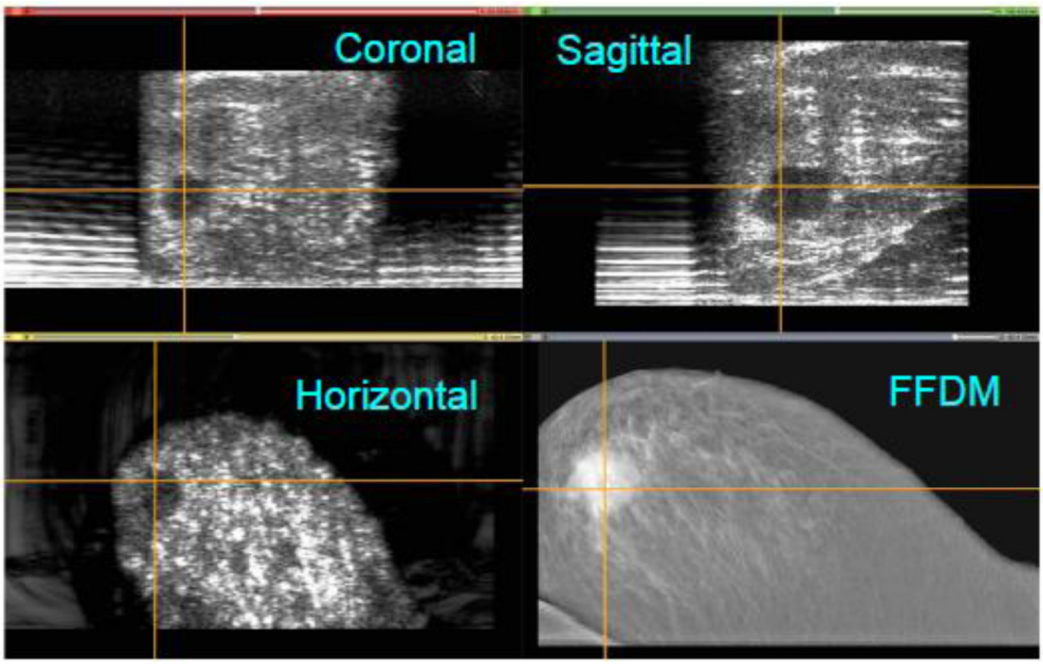

Figure 10.

Co-registration of the full-field digital mammogram (FFDM) in the horizontal plane and the automated breast ultrasound (ABUS) images in the horizontal, coronal and sagittal planes. A malignant lesion has been highlighted by cross hairs in the ABUS views, and is clearly is co-registered in the FFDM image. Note that for the ABUS images, the sagittal plane view is the acquired image, whereas the coronal and horizontal plane views have been reconstructed.

Table 1

Definition of parameters recommended by the Food & Drug Administration (FDA) to judge the quality of full-field digital mammography (FFDM) images. Source: www.fda.gov/RegulatoryInformation/Guidances/ucm107552.htm

Parameter	Definition
Breast positioning	Assess coverage of the breast on cranio-caudal (CC) and medio-lateral oblique (MLO) views
Exposure	Assess visualization of the adipose and fibroglandular tissues and visualization of breast tissue underlying the pectoralis muscle
Breast compression	Assess overlapping breast structures, uniformity of exposure of fibroglandular tissues, adequacy of penetration of thicker portions, exposure of thinner areas and motion unsharpness
Image contrast	Assess differentiation of subtle tissue density differences
Sharpness	Assess the edges of fine linear structures, tissue borders and benign calcifications
Tissue visibility	Assess the tissue visibility on the skin line
Noise	Assess noise obscuring breast structures or suggestive of structures not actually present
Artifacts	Assess artifacts due to image processing, detector failure and other factors external to the breast
Image quality	Assess the overall clinical image quality

Table 2

Mean values for the 58 subjects (51 healthy volunteers and 7 patients), including age, 12 full-field digital mammography (FFDM) parameters as assessed by the radiologist (QSH), and the time taken by the radiographer with each subject in the image acquisition room.

Parameter		Mean value
Age (years)		50.4
Breast positioning	Cranio-caudal	−0.10
	Medio-lateral oblique	−0.47
Exposure	Adipose	−0.31
	Fibroglandular	−0.36
	Pectoralis	−0.50
Breast compression		−0.48
Image contrast		−0.95
Sharpness		−0.97
Tissue visibility		−0.98
Noise		−0.03
Artifacts		−0.50
Image quality		−0.93
Time (min:sec)		10:57

Table 3

Radiological findings by the radiologist (QSH) for the 7 patients, including breast density (BI-RADS 1 to 4). These recorded comments were based on the full-field digital mammography (FFDM) and automated breast ultrasound (ABUS) images generated by the Aceso system.

Patient	Density	FFDM findings	ABUS findings
1	2	Irregular mass (3 cm) in R breast with distortion, consistent with invasive carcinoma. Microcalcifications seen in close proximity.	Ultrasound confirms suspicious mass, with posterior acoustic enhancement. The FFDM and ABUS images are complimentary.
2	2	Irregular mass (2 × 1.8 cm) in L breast with architectural distortion. No associated microcalcifications seen.	Ultrasound does not demonstrate the lesion well.
3	4	Small dense breasts with no discrete spiculations or architectural distortion. No malignant microcalcifications.	Ultrasound shows normal tissue with no visible solid or cystic masses.
4	3	Large (2.5 cm) lobulated mass seen in L breast. No microcalcifications or adenopathy seen.	Although seen, ultrasound did not help to characterize the lesion.
5	2	Ill-defined increase in density in L breast with some architectural distortion seen but no calcification.	No lesion identified on ultrasound.
6	2	Spiculated subareolar mass (1-2 cm) seen in L breast which is consistent with invasive carcinoma.	Ultrasound confirmed hypoechoic irregular lesion consistent with mammographic findings.
7	3	Spiculated lesion in upper outer quadrant of R breast, consistent with invasive carcinoma. No microcalcifications seen.	ABUS showed a hypoechoic lesion with confirmation of associated abnormal acoustic shadowing.